The Journal of Neuroscience, July 1, 2000, 20(13):4912–4921

# Active Zones on Motor Nerve Terminals Contain α3β1 Integrin

**Monroe W. Cohen,[1] Benjamin G. Hoffstrom,[2] and Douglas W. DeSimone[2]**

*[1]Department of Physiology, McGill University, Montreal, Quebec Canada H3G 1Y6, and [2]Department of Cell Biology, University of Virginia, Charlottesville, Virginia 22908*

Active zones are the sites along nerve terminals where synaptic vesicles dock and undergo calcium-dependent exocytosis during synaptic transmission. Here we show, by immunofluorescent staining with antibodies generated against *Xenopus laevis* integrins, that α3β1 integrin is concentrated at the active zones of *Xenopus* motor nerve terminals. Because integrins can link extracellular matrix molecules to cytoskeletal elements and participate in the formation of signaling complexes, the localization of integrin at active zones suggests that it may play a role in the adhesion of the nerve terminals to the synaptic basal lamina, in the formation and maintenance of active zones, and in some of the events associated with calcium-dependent exocytosis of neurotransmitter. Our findings also indicate that the integrin composition of the terminal Schwann cells differs from that of the motor nerve terminals, and this may account at least in part for differences in their adhesiveness to the synaptic basal lamina.

*Key words: active zones; α3β1 integrin; motor nerve terminals; terminal Schwann cells;* Xenopus laevis*; neuromuscular junction; neurotransmitter release*

Integrins are a large family of transmembrane heterodimers. They can interact with and establish a link between extracellular matrix and cytoskeletal molecules and can also participate in the generation of signaling cascades. The expression of the individual α and β subunits that combine to form the integrin molecule depends on cell type and is developmentally regulated. Different integrins have different affinities for individual matrix and cytoskeletal proteins and initiate different signaling cascades (Hynes, 1992; Clarke and Brugge, 1995; Aplin et al., 1998).

Integrins are differentially expressed in different regions of the nervous system (Pinkstaff et al., 1999) and have been implicated in its development and operation. Developmental events involving integrins include axonal growth and guidance (Dodd and Jessell, 1988; Reichardt and Tomaselli, 1991), cell migration (Kil et al., 1996), and the clustering of acetylcholine receptors (AChRs) during formation of the neuromuscular junction (Anderson et al., 1996; Martin and Sanes, 1997; Burkin et al., 1998). Operationally, integrins have been implicated in the stabilization of long-term potentiation (Bahr et al., 1997; Stäubli et al., 1998). The latter role may involve the integrin subunits α8 and β8 that are concentrated at the postsynaptic densities of dendritic spines (Einheber et al., 1996; Nishimura et al., 1998). At neuromuscular junctions, integrin subunits α1, α3, α7, α9, αV, and β1 have been detected (Bozyczko et al., 1989; Belkin et al., 1996; Martin et al., 1996). After denervation, the α7 subunit remains at the neuromuscular junction, indicating that it is associated with the postsynaptic membrane (Martin et al., 1996).

Besides having a postsynaptic localization, integrins can also be present presynaptically. The β8 subunit is associated with some of the axon terminals in the rat hippocampus (Nishimura et al., 1998). The α1 integrin subunit at the neuromuscular junction is no longer detected after denervation, thereby suggesting that it may normally be present on intact motor nerve terminals (Martin et al., 1996). In addition, a polyclonal anti-integrin antibody and a peptide that interferes with integrin binding to extracellular matrix molecules have been found to inhibit stretch-enhanced release of neurotransmitter at the frog neuromuscular junction (Chen and Grinnell, 1995). Such findings are consistent with the possibility that integrins are present on motor nerve terminals and on other nerve endings as well and play a role in neurotransmitter release.

In the present study we have used antibodies generated against *Xenopus laevis* integrins to examine, by immunofluorescent staining, the localization of integrins at *Xenopus* neuromuscular junctions. These synapses are particularly advantageous for assessing precise localization because the junctional folds and apposed active zones have a characteristic pattern of distribution, and the presynaptic and postsynaptic elements can be separated from each other. Our results reveal that the α3β1 integrin is present on the motor nerve terminals and concentrated at their active zones.

## MATERIALS AND METHODS

*Animals and surgical procedures. Xenopus laevis* frogs, weighing <2 gm, were anesthetized in 0.5 mg/ml tricaine methanesulphonate. The sartorius muscles were removed and stored at low temperature (4–6°C) in a solution consisting of 67% (v/v) L-15 and 1% (v/v) goat serum (Life Technologies, Burlington, ON, Canada). To denervate sartorius muscles, animals were anesthetized, and their left spinal nerve was resected shortly after its exit from the spinal cord. Care was taken not to injure any blood vessels. Muscles were removed 3 or 6 d later.

*Fluorescent staining and imaging.* Sartorius muscles were stained alive at low temperature (4–6°C). The standard bathing solution consisted of 67% (v/v) L-15 and 1% (v/v) goat serum. Muscles were exposed to the primary and secondary antibodies for at least 2 hr and were rinsed several times over a period of at least 20 min after each antibody. Fluorescent toxins were usually included with the secondary antibody but were sometimes used earlier in the staining protocol. After being stained the muscles were rinsed with 67% L-15 and fixed with 2% formaldehyde for at least 1 hr. For some experiments, the muscles were treated with 1 mg/ml collagenase (Life Technologies) in 67% L-15 for 1 hr at room

Received Feb. 25, 2000; revised April 6, 2000; accepted April 10, 2000.

This work was supported by a grant to M.W.C. from the Medical Research Council of Canada and by grants to D.W.D. from the United States Public Health Service (HD26402 and HD01104). D. McDonald and T. Inoue provided expert technical assistance. We thank S. Carbonetto for monoclonal antibody 8C8, S. S. Carlson for the anti-SV2 antibody, and O. T. Jones for RωCT.

Correspondence should be addressed to M. W. Cohen, Department of Physiology, McGill University, 3655 Drummond Street, Montreal, Quebec, Canada H3G 1Y6. E-mail: monroe@med.mcgill.ca.

**Table 1. Integrin immunofluorescence along muscle cells[a]**

| Integrin | mAb | Dilution | Synaptic bands | Terminal Schwann cells | Costameres | Satellite cells |
|---|---|---|---|---|---|---|
| $\alpha3\beta1$ | P2A5 | 1/100 | ++ | + | + | + |
| | | 1/1000 | + | − | − | − |
| $\alpha3\beta1$ | P7A12 | 1/100 | ++ | ++ | ++ | ++ |
| | | 1/1000 | +/− | +/− | +/− | +/− |
| $\alpha5\beta1$ | P2A7 | 1/100 | +/− | + | +/− | + |
| $\alpha V\beta3$ | P3C12 | 1/100 | − | − | − | − |
| $\beta1$ | 8C8 | 1/100 | ++ | ++ | ++ | ++ |
| | | 1/1000 | +/− | + | +/− | + |

[a]Relative intensities of the immunofluorescence were assessed by eye and are denoted as bright (++), moderate (+), faint (+/−), or undetectable (−).

temperature (22–25°C) before fixation. The collagenase solution also contained 1.5 μM tetrodotoxin (Sigma, St. Louis, MO). Some fixed muscles were subsequently rinsed with 67% L-15, permeabilized with 1% Triton X-100 (30 min at 4–6°C), and stained for the synaptic vesicle protein SV2. The staining protocol after fixation and permeabilization was the same as described for the initial staining of living muscles. After staining and rinsing, the muscles were stored in the fixative.

Individual muscle fibers were isolated from the fixed muscles. Typically, each of the isolated fibers contained two to three neuromuscular junctions, but no attempt was made to include the myotendinous junction. At least 20 muscle fibers from each muscle were mounted on glass slides. The mounting medium consisted of 10 mg/ml *p*-phenylenediamine, 10 mM sodium carbonate, and 90% (v/v) glycerol. The slides were examined on a Zeiss IM35 microscope equipped with appropriate oil-immersion objectives and filters for viewing fluorescein, rhodamine and Cy3, and aminomethylcoumarin (AMCA) fluorescence as well as phase contrast. High (100× objective) and low (25× objective) magnification photographs were taken with T-MAX 3200 Kodak (Eastman Kodak, Rochester, NY) film. The negatives were digitized on an MCID-M4 imaging system (Imaging Research, St. Catharine's, Ontario, Canada), and figures were prepared using Adobe PhotoShop.

The following anti-*Xenopus* integrin mouse monoclonal antibodies (mAbs) were prepared and characterized (see below): P2A5 and P7A12 directed against $\alpha3\beta1$ integrin; P2A7 against a5$\beta1$ integrin; and P3C12 against $\alpha V\beta3$ integrin. Each antibody was tested on three or more muscles at a dilution of 1/100 (6–14 μg/ml), and some were tested at 10-fold lower concentrations as well (Table 1). Another mAb, 8C8, against the *Xenopus* $\beta1$ integrin subunit (Gawantka et al., 1992), was a gift from S. Carbonetto (McGill University, Montreal, Quebec, Canada). A mAb against the synaptic vesicle protein SV2 was a gift from S. S. Carlson (University of Washington, Seattle, WA). The anti-integrin antibodies were stained with affinity-purified, goat anti-mouse antibodies conjugated with either Cy3 (Jackson ImmunoResearch, West Grove, PA) or with fluorescein (Molecular Probes, Eugene, OR). AChRs were stained with fluorescein- or rhodamine-conjugated α-bungarotoxin (FαBT, RαBT; Molecular Probes). N-type calcium channels were stained with rhodamine-conjugated ω-conotoxin (RωCT), a gift from O. T. Jones (University Health Network, Toronto, Ontario, Canada). The anti-SV2 mAb was stained with an AMCA-conjugated secondary antibody (Jackson ImmunoResearch). All fluorescent secondary antibodies were used at 10 μg/ml.

*Characterization of anti-integrin monoclonal antibodies. Xenopus* S3–1 cells represent a clonal cell line that was isolated from trypsinized dorsal explants of stage 18 neurulae cultured in 61% L-15 media containing 10% FBS. These cells were selected for use as immunogen on the basis of their adhesion to a variety of extracellular matrix substrates, including fibronectin, and for the presence of multiple integrins on their cell surface. Mice were immunized with live S3–1 cells, and anti-*Xenopus* mAbs were generated using the methods for hybridoma fusion and screening described by Wayner and Carter (1987). Details regarding the characterization of the S3–1 cells and the complete hybridoma screen for *Xenopus* integrins will be reported elsewhere (B. G. Hoffstrom and D. W. DeSimone, unpublished observations).

Four mAbs (P2A5, P7A12, P2A7, P3C12) from this screen were used in the current study and characterized by immunoprecipitation and Western blot analyses. Unlabeled S3–1 cells and S3–1 cells surface-labeled with sulfosuccinimidyl-6-(biotinamido) hexanoate (NHS-LC-Biotin; Pierce, Rockford, IL) were washed in PBS and extracted in IP buffer (1% NP-40, 10 mM Tris, pH 7.75, 150 mM NaCl, 1 mM PMSF, 2 μg/ml aprotinin, 2 μg/ml leupeptin, and 1 μg/ml pepstatin A). Integrins were immunoprecipitated from biotin-labeled and unlabeled cell extracts ($1.0 \times 10^5$ cell equivalents) using mAbs (2 μg/ml) and goat anti-mouse coupled agarose (Sigma) as described in Hens and DeSimone (1995). Western blotting was performed using standard techniques (Towbin et al., 1979). Biotinylated proteins were detected with 0.2 μg/ml streptavidin-HRP (Pierce). Unlabeled immunoprecipitated proteins were detected using HRP-conjugated goat anti-rabbit secondary antibodies (1:10,000; Jackson ImmunoResearch). All extracts were run under nonreducing conditions with the exception of extracts probed with anti-*Xenopus* $\alpha5$ polyclonal antibody (Joos et al., 1995), which recognizes reduced antigen.

## RESULTS

### Characterization of anti-*Xenopus* integrin monoclonal antibodies

The specificities of the *Xenopus*-specific anti-integrin mAbs were established by immunoprecipitation and Western blot analyses of

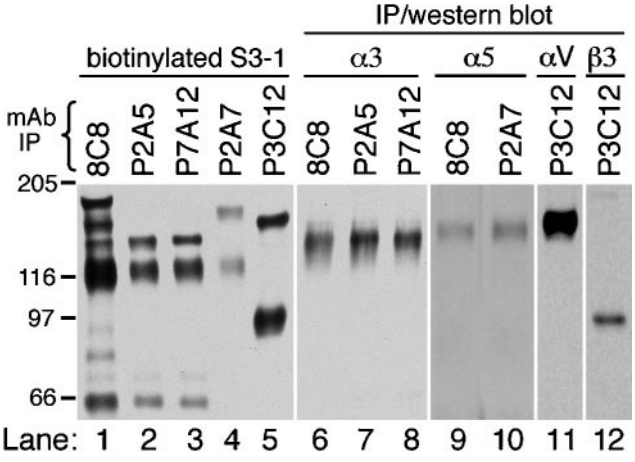


*Figure 1.* Specificity of mAbs directed against *Xenopus* integrins. For *lanes 1–5*, *Xenopus* S3–1 cells were labeled by cell-surface biotinylation, extracted in IP buffer, and immunoprecipitated using the following mAbs: 8C8 (anti-$\beta1$; Gawantka et al., 1992), P2A5 and P7A12 (anti-$\alpha3\beta1$), P2A7 (anti-$\alpha5\beta1$), and P3C12 (anti-αV). Immunoprecipitated proteins were separated by SDS-PAGE, transferred to nitrocellulose, and probed with streptavidin-HRP. For lanes 6–12, unlabeled S3–1 cell extracts were immunoprecipitated using the mAbs indicated and Western-blotted using HRP-conjugated secondary antibodies. Western blots were probed with subunit-specific polyclonal antibodies directed against $\alpha3$ (Ab D3FAP; Meng et al., 1997), $\alpha5$ (Ab 881; Joos et al., 1995), αV (Ab 1930; Chemicon, Temecula, CA), and $\beta3$ (Ab VA-28; D. G. Ransom, M. D. Hens, and D. W. DeSimone, unpublished observations). All immunoprecipitations were run on 6.5% SDS-PAGE gels under nonreducing conditions (with the exceptions of lanes 9–10, which were run under reducing conditions). The <66 kDa band observed in the 8C8, P2A5, and P7A12 immunoprecipitates of biotin-labeled cells (*lanes 1–3*) corresponds to a proteolytic fragment of $\alpha3$ reported previously (Gawantka et al., 1994; Meng et al., 1997).

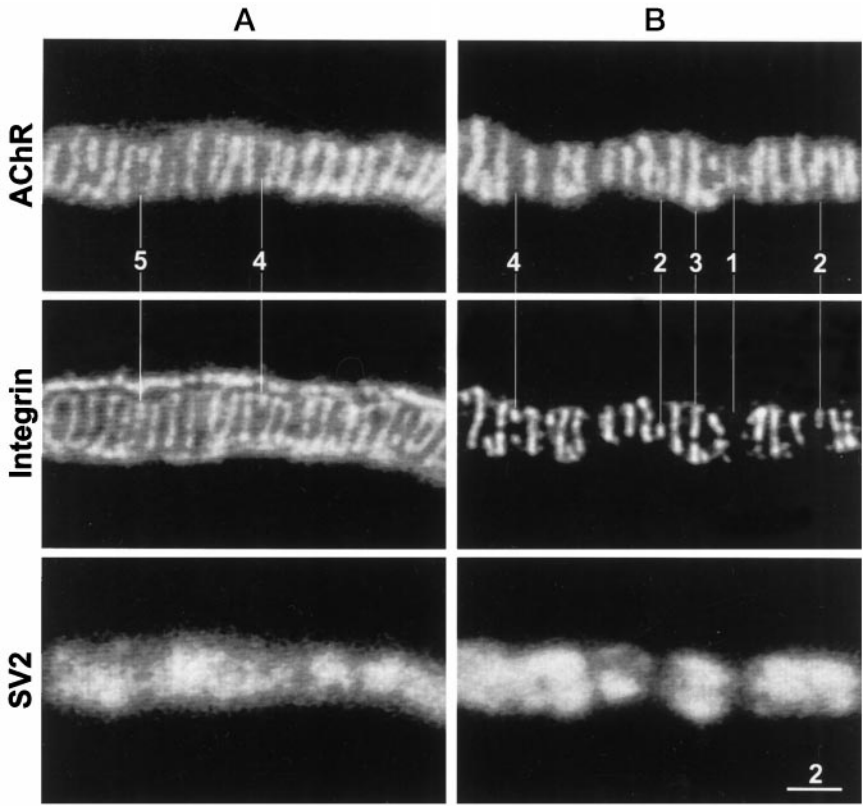


*Figure 2.* Face views of two neuromuscular junctions (*A, B*) stained for AChRs (*top panels*), $\alpha3\beta1$ integrin (*middle panels*), and synaptic vesicle protein SV2 (*bottom panels*). The integrin in this and other figures was stained with mAb P2A5. Note extensive correspondence as well as subtle differences between the transverse bands of AChR fluorescence and of integrin immunofluorescence. The differences, marked by the numbered lines, include: (1) a faint AChR band without a corresponding integrin band, (2) integrin bands that are shorter than the corresponding AChR bands, (3) an integrin band that is segmented, whereas its corresponding AChR band is not, (4) short integrin bands without corresponding AChR bands, and (5) an integrin band that is longer than its corresponding AChR band. Integrin immunofluorescence that outlines the neuromuscular junction in *A* but not in *B* is associated with the outer surface of the terminal Schwann cell. Scale bar, 2 $\mu$m.

*Xenopus* S3–1 cell extracts. S3–1 represents a clonal line of cells obtained from dorsal explants of neurula stage embryos. As shown in Figure 1, immunoprecipitation of biotin-labeled S3–1 cells with an anti-$\beta1$ subunit mAb (8C8) revealed a prominent $\beta1$ band (118 kDa) and several associated $\alpha$ subunits (~140–165 kDa), indicating that these cells express a number of distinct integrin $\beta1$ heterodimers at their cell surface (lane 1). The P2A5 and P7A12 mAbs immunoprecipitated the $\beta1$ subunit and a single 140 kDa $\alpha$ subunit (lanes 2 and 3), which corresponds to the size reported previously for *Xenopus* $\alpha3$ (Meng et al., 1997). When unlabeled S3–1 cells were immunoprecipitated with 8C8, P2A5, or P7A12 and the precipitates were Western-blotted using a polyclonal antibody directed against *Xenopus* $\alpha3$, only the 140 kDa subunit was detected (lanes 6–8). These data confirm that the P2A5 and P7A12 mAbs recognize a single $\beta1$ heterodimer, which corresponds to the $\alpha3\beta1$ integrin complex.

A similar approach was used to confirm the specificities of the anti-$\alpha5$ mAb P2A7 and the anti-$\alpha V\beta3$ mAb P3C12. P2A7 immunoprecipitated a 155/118 kDa complex from biotinylated S3–1 cells (Fig. 1, *lane 4*). Western blots of 8C8 and P2A7 immunoprecipitates probed with an anti-$\alpha5$ polyclonal antibody detected only the reduced $\alpha5$ subunit that runs at 145 kDa (Fig. 1, *lanes 9, 10*). In contrast, P3C12 recognized a single non-$\beta1$-containing heterodimer (Fig. 1, *lane 5*). The subunit identity of this 150/90 kDa $\alpha V\beta3$ complex was confirmed by Western blot using anti-$\alpha V$ and anti-$\beta3$ polyclonal antibodies (Fig. 1, *lanes 11, 12*).

### Staining patterns with mAb P2A5 (anti-$\alpha3\beta1$ integrin)

Figure 2 shows face views of portions of two different neuromuscular junctions stained for AChRs, $\alpha3\beta1$ integrin, and synaptic vesicle membrane protein SV2. The AChR staining pattern consisted of a characteristic series of bright, transversely oriented bands as well as fainter fluorescence between the bands. The bright bands are the sites where the postsynaptic membrane invaginates to form the junctional folds (Anderson and Cohen, 1974). The corresponding integrin immunofluorescence also consisted of transversely oriented bands, almost all of which were in spatial register with the AChR bands. However, the pattern of integrin immunofluorescence was not identical to that of the AChR stain. At some neuromuscular junctions the outer surface of the terminal Schwann cells, which cover the nonsynaptic portion of the nerve terminal membrane, was also stained. This immunofluorescence appeared as an outlining of the neuromuscular junction (Fig. 2*A*) and also revealed the expanded Schwann cell body as well as regions where the terminal Schwann cell (and its associated axon terminal) bridged neighboring branches of the same neuromuscular junction (data not shown). By contrast, the SV2 immunofluorescence was confined entirely to the synaptic portions of the nerve terminals.

Although there was extensive congruity between the AChR bands and the integrin bands, subtle differences were also observed. Examples of such differences are indicated by the numbered lines in Figure 2. Line 1 points to a short AChR band with no corresponding integrin stain. Some AChR bands were longer than the corresponding integrin bands (lines 2), and sometimes an integrin band was segmented, whereas the corresponding AChR band was not (line 3). Occasionally short integrin bands had no corresponding AChR fluorescence (lines 4), and some integrin bands were longer than the corresponding AChR band (line 5).

In side views of neuromuscular junctions (Fig. 3), the AChR stain consisted of a thin line with short, periodic, perpendicular extensions. The latter are the sites where the postsynaptic membrane invaginates to form the junctional folds, whereas the thin continuous horizontal line of AChR fluorescence is attributable

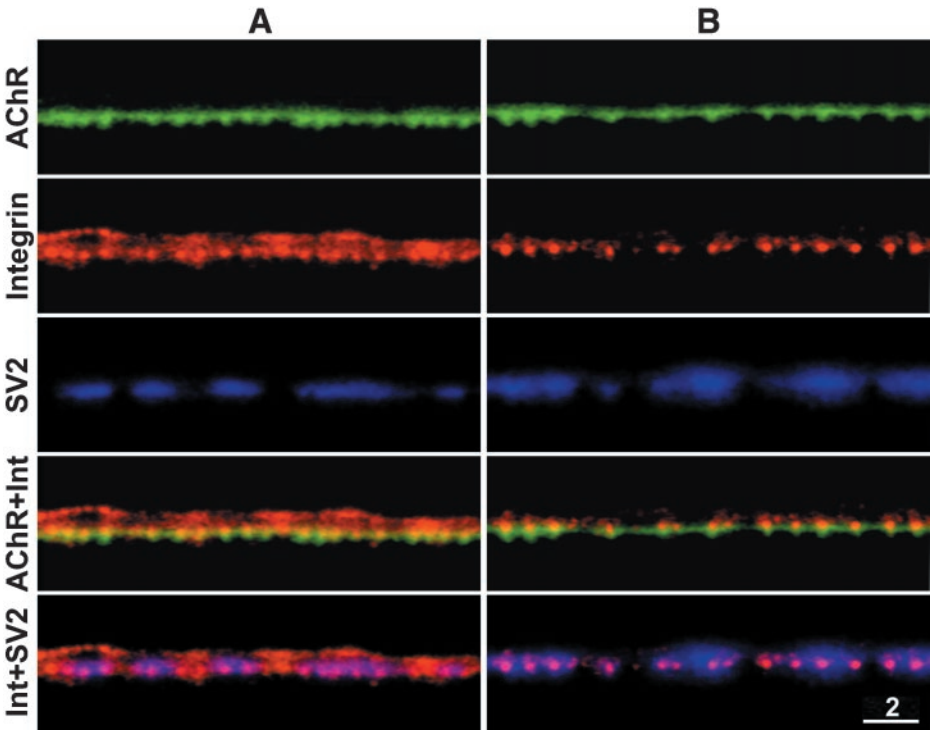


*Figure 3.* Side views of two neuromuscular junctions (*A, B*) stained for AChRs (*top panels*), $\alpha 3\beta 1$ integrin (*second panels*), and SV2 (*third panels*). The short periodic downward extensions of AChR fluorescence are the sites where the postsynaptic membrane invaginates to form the junctional folds. Merged images indicate that the bright dots of integrin immunofluorescence were aligned with the tops of the junctional folds ( *fourth panels*) and with the synaptic side of the motor nerve terminals (*bottom panels*). The outer surface of the Schwann cell was revealed by the integrin immunofluorescence in *A* but not in *B*. Scale bar, 2 $\mu$m.

to the presence of AChRs in the noninvaginated portion of the postsynaptic membrane between the junctional folds (Anderson and Cohen, 1974). The corresponding integrin immunofluorescence consisted of a prominent series of bright dots. As expected from the face views, almost all of the bright integrin dots were in spatial register with the junctional folds. Significantly, they overlapped with the tops of the junctional folds and with the synaptic side of the motor nerve terminal. This could mean that the integrin is concentrated in the postsynaptic membrane at the tops of the junctional folds and/or in the motor nerve terminal membrane at the active zones, which are known to be spatially aligned with the junctional folds (Couteaux and Pécot-Dechavassine, 1970; Dreyer et al., 1973). In some cases, there was additional integrin immunofluorescence close to, but in some regions clearly separated from, the nonsynaptic side of the SV2 immunofluorescence (Fig. 3*A*). This separation was greatest at the Schwann cell body (data not shown), consistent with our observations of face views that $\alpha 3\beta 1$ integrin is present on the outer surface of the terminal Schwann cells. Additional integrin stain was observed in SV2-deficient regions (Fig. 3*A*) and may reflect sites where the Schwann cell extends processes that partially enwrap the nerve terminal (Birks et al., 1960a; Astrow et al., 1998).

In addition to its presence at neuromuscular junctions, integrin immunofluorescence was observed elsewhere along the muscle cells. This consisted of faint immunofluorescence along the entire surface of the muscle cells and brighter immunofluorescence localized at costameres and satellite cells (see Fig. 7*A*). The intensity of the integrin immunofluorescence at these sites, like that at the terminal Schwann cells, was variable. When the integrin stain at terminal Schwann cells was faint or undetectable, so too was the integrin stain at neighboring costameres and satellite cells, even though the synaptic integrin bands were relatively bright, and the SV2 immunofluorescence was also bright (Fig. 2*B*). Presumably such cases involved teased muscle cells whose neuromuscular junctions were originally positioned more deeply within the whole muscle so that during the staining protocol they were exposed to a lower concentration of antibody than the more superficial ones. In support of this notion, when the staining protocol was performed with a tenfold lower concentration of mAb P2A5 there was often no detectable immunofluorescence at terminal Schwann cells, costameres, and satellite cells even though integrin bands, in spatial register with the AChR bands, were still observed at neuromuscular junctions (Table 1). This preferential staining of the synaptic membrane may reflect a higher affinity of the antibody for the synaptic integrin and/or a greater concentration of integrin at the synaptic sites than at Schwann cells, costameres, and satellite cells.

### Staining patterns with other anti-integrin mAbs

The staining patterns obtained with mAb P7A12, which like mAb P2A5 is directed against $\alpha 3\beta 1$ integrin, were similar to those described above. However, as summarized in Table 1, some differences were apparent in the relative intensities of the immunofluorescence. Generally, the mAb P7A12 immunofluorescence at terminal Schwann cells, costameres, and satellite cells was brighter than that seen with mAb P2A5 and sometimes resulted in bleedthrough into the fluorescein optics. Furthermore, at a 10-fold lower concentration of mAb P7A12, the synaptic bands tended to be fainter than those seen with mAb P2A5. It may be that mAbs P2A5 and P7A12 are reactive with different epitopes on the $\alpha 3\beta 1$ integrin molecule, and their access to these epitopes varies at different cellular sites depending on the associated extracellular matrix molecules.

mAb P2A7, which is directed against $\alpha 5\beta 1$ integrin, stained synaptic bands and costameres only faintly, whereas the terminal Schwann cells and satellite cells appeared somewhat brighter (Table 1). Because immunofluorescent staining did not detect the $\alpha 5$ subunit at human neuromuscular junctions (Martin et al., 1996), the presence of some $\alpha 5\beta 1$ integrin at *Xenopus* neuromuscular junctions may be attributable to species differences, but the

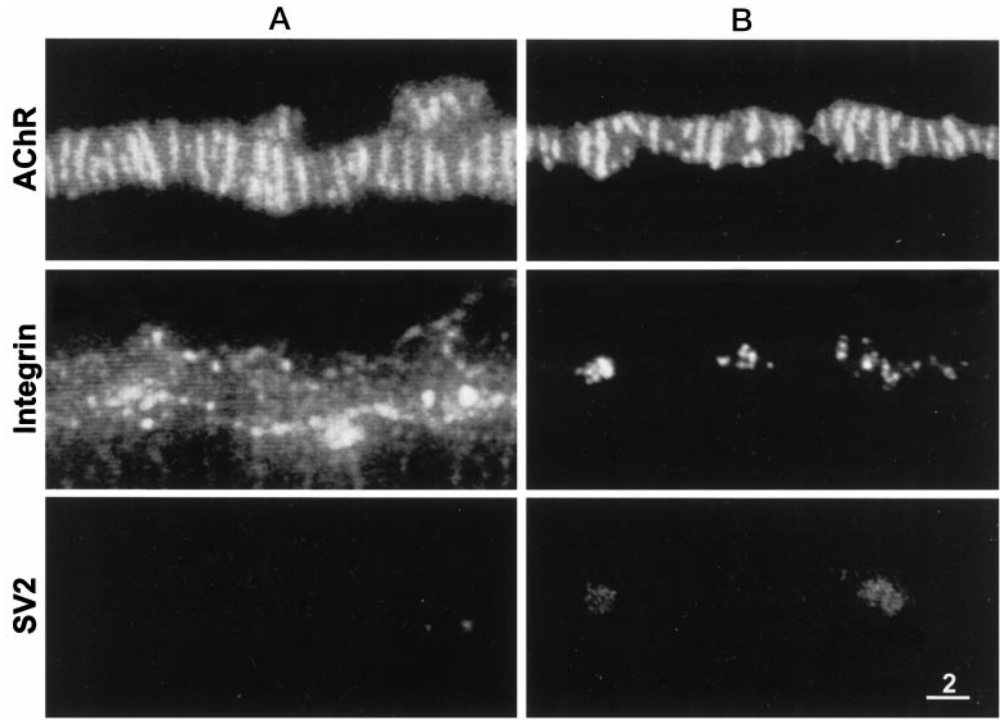


*Figure 4.* Disappearance of synaptic bands of $\alpha 3\beta 1$ integrin after denervation. *A,* Denervated for 6 d. Transverse bands of AChRs (*top panel*) are apparent, but corresponding bands of integrin immunofluorescence (*middle panel*) are not, and SV2 immunofluorescence (*bottom panel*) is undetectable. The regions of bright integrin immunofluorescence may reflect changes in the Schwann cell in response to degeneration of the motor nerve terminals. *B,* Denervated for 3 d. There are no transverse integrin bands. Instead there are some isolated sites of integrin stain and some faint SV2 immunofluorescence. These sites are probably portions of degenerating nerve terminals that have not yet been phagocytosed. Scale bar, 2 $\mu$m.

results in both species suggest that this integrin is poorly represented in the presynaptic and postsynaptic membranes of the neuromuscular junction.

Staining the sartorius muscle for $\alpha V\beta 3$ integrin with mAb P3C12 resulted in no detectable immunofluorescence at all (Table 1), even though it is effective in staining adult *Xenopus* tissues such as skin as well as embryonic cells (data not shown). The $\alpha V$ subunit is present at the human neuromuscular junction (Martin et al., 1996), but it is not known if the heterodimer $\alpha V\beta 3$ is present there. Myoblasts express the $\alpha V\beta 3$ integrin, but this expression is downregulated during their differentiation (Blaschuk et al., 1997).

The staining pattern obtained with mAb 8C8, which is directed against the $\beta 1$ subunit, was similar to that obtained with mAbs P2A5 and P7A12. However, the immunofluorescence at all sites was often so bright that it resulted in bleedthrough into the fluorescein optics. With a further 10-fold dilution, the resulting mAb 8C8 immunofluorescence was brighter on the terminal Schwann cells than at the synaptic bands (Table 1). Overall then, although the staining patterns obtained with the two anti-$\alpha 3\beta 1$ mAbs (P2A5, P7A12) and with the anti-$\beta 1$ mAb (8C8) were similar, the synaptic bands of integrin were stained most preferentially by mAb P2A5. Accordingly, mAb P2A5 was used most extensively in subsequent experiments to assess the presynaptic versus postsynaptic location of these bands.

### Staining patterns in denervated muscle

After denervation, motor nerve terminals degenerate and are phagocytosed by the terminal Schwann cells that remain at the neuromuscular junctions even after all motor nerve terminal remnants have been eliminated (Birks et al., 1960b; Ko, 1981). It follows that if the synaptic bands of $\alpha 3\beta 1$ integrin are associated exclusively with the active zones of motor nerve terminals, denervation should lead to their disappearance. This prediction was tested with mAb P2A5 (Fig. 4) as well as with mAbs P7A12 and 8C8 (data not shown), and the results were similar. As expected from previous work (Cohen et al., 1991) denervated neuromuscular junctions, 6 d after cutting the nerve (Fig. 4*A*), still exhibited the characteristic transverse AChR bands and had no detectable SV2 immunofluorescence. Significantly, there were no bright bands of integrin immunofluorescence colocalized with the AChR bands. Instead there was faint integrin immunofluorescence either with a bright outlining similar in appearance to that seen at normal neuromuscular junctions (see Fig. 2*a*) or with irregular bright regions (Fig. 4*A*). The latter pattern was not observed at innervated neuromuscular junctions and may reflect changes in the terminal Schwann cells in response to the degeneration of the nerve terminals. The source of the faint integrin immunofluorescence could be the Schwann cell or the postsynaptic membrane. At other denervated neuromuscular junctions (which presumably originated from deeper within the whole muscle) there was no integrin immunofluorescence at all. Even 3 d after cutting the nerve, most of the neuromuscular junctions were completely devoid of synaptic integrin bands, and their SV2 immunofluorescence was relatively faint and sparse or undetectable. Some isolated patches of integrin immunofluorescence were observed, and these may have been associated with remnants of nerve terminal that were not yet phagocytosed (Fig. 4*B*).

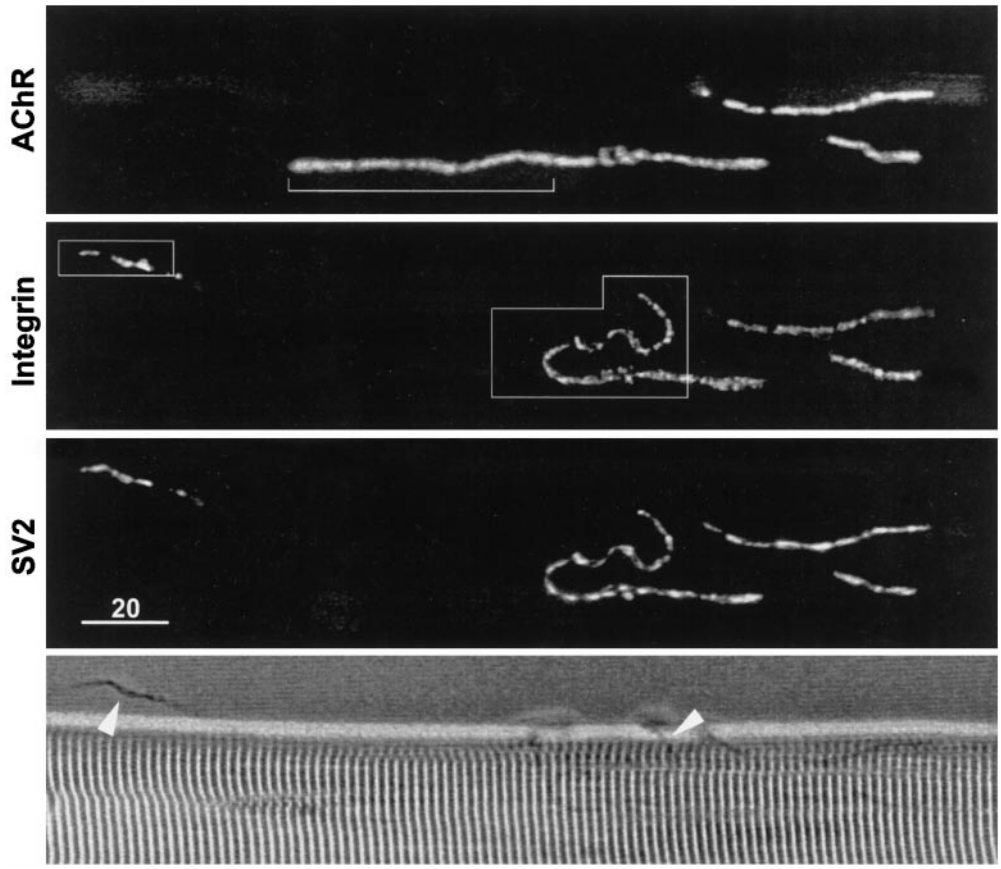


*Figure 5.* Low-magnification view of a neuromuscular junction treated with collagenase. Comparison of the AChR fluorescence (*top panel*) and the SV2 immunofluorescence (*third panel*) reveals that the motor nerve terminal was displaced from a portion of the postsynaptic membrane (*top panel, bracket*). Displaced nerve terminal branches are also apparent in the phase-contrast image (*bottom panel, arrowheads*). The $\alpha 3\beta 1$ integrin immunofluorescence (*second panel*) is codistributed with the nerve terminal branches and is not detectable at the portion of postsynaptic membrane that lacks nerve terminal. Framed portions of the field are shown at higher magnification in Figure 6. Scale bar, 20 $\mu$m.

## Presynaptic location of synaptic integrin bands

The absence of synaptic integrin bands at denervated neuromuscular junctions suggests that, at innervated neuromuscular junctions, they are associated with active zones on the motor nerve terminals. An additional possibility is that they are associated with the postsynaptic membrane at the tops of the junctional folds, but their survival there requires the presence of intact motor nerve terminals. To assess whether the synaptic integrin bands are associated with motor nerve terminals, muscles were treated with collagenase to displace the nerve terminals from their neuromuscular junctions. Such enzymatic treatment, by digesting the synaptic basal lamina, weakens the adhesion of the motor nerve terminals to their muscle cells and makes them susceptible to displacement (McMahan et al., 1972; Betz and Sakmann, 1973). The treatment also leads to changes in the orientation of the active zones and to their disruption (Nystrom and Ko, 1988).

Figure 5 shows a low-magnification view of a neuromuscular junction after enzymatic treatment. The AChR fluorescence (*top panel*) reveals the location of the postsynaptic membrane, and the SV2 immunofluorescence (*third panel*) reveals that the motor nerve terminal was partially displaced from the postsynaptic membrane. A short length of displaced nerve terminal is seen on the left side of the figure, and a longer length is seen on the right. Portions of the displaced motor nerve terminal are also apparent in the phase-contrast image (*bottom panel*). Significantly, the integrin immunofluorescence (obtained with mAb P2A5; *second panel*) was associated with the displaced nerve terminal, whereas the portion of postsynaptic membrane that lacked motor nerve terminal (bracket in *top panel*) also lacked integrin stain. This absence of integrin immunofluorescence along nerve terminal-free portions of postsynaptic membrane was also observed in cases in which the surrounding costameres and neighboring satellite cells had relatively bright integrin immunofluorescence (see Fig. 7).

Figure 6 shows higher magnification views of the framed areas in Figure 5. At the portion of neuromuscular junction that remained intact the synaptic integrin bands had become disorganized. Many of the individual integrin bands were no longer spatially aligned with the transversely oriented AChR bands, and some even had a horizontal orientation. In addition, the integrin bands were less numerous than the AChR bands. Such changes are similar to those that have been described for active zones examined by electron microscopy after enzymatic treatment (Nystrom and Ko, 1988). Also in agreement with the electron microscopic observations of enzyme-treated active zones, the degree of these changes varied at different neuromuscular junctions from almost normal in appearance to an almost total lack of integrin bands.

Integrin bands having a variety of orientations were also observed on the displaced motor nerve terminals. As seen in the examples of Figures 6 and 7, the integrin bands on the displaced motor nerve terminals had an appearance that was essentially similar to the appearance of the integrin bands at intact portions

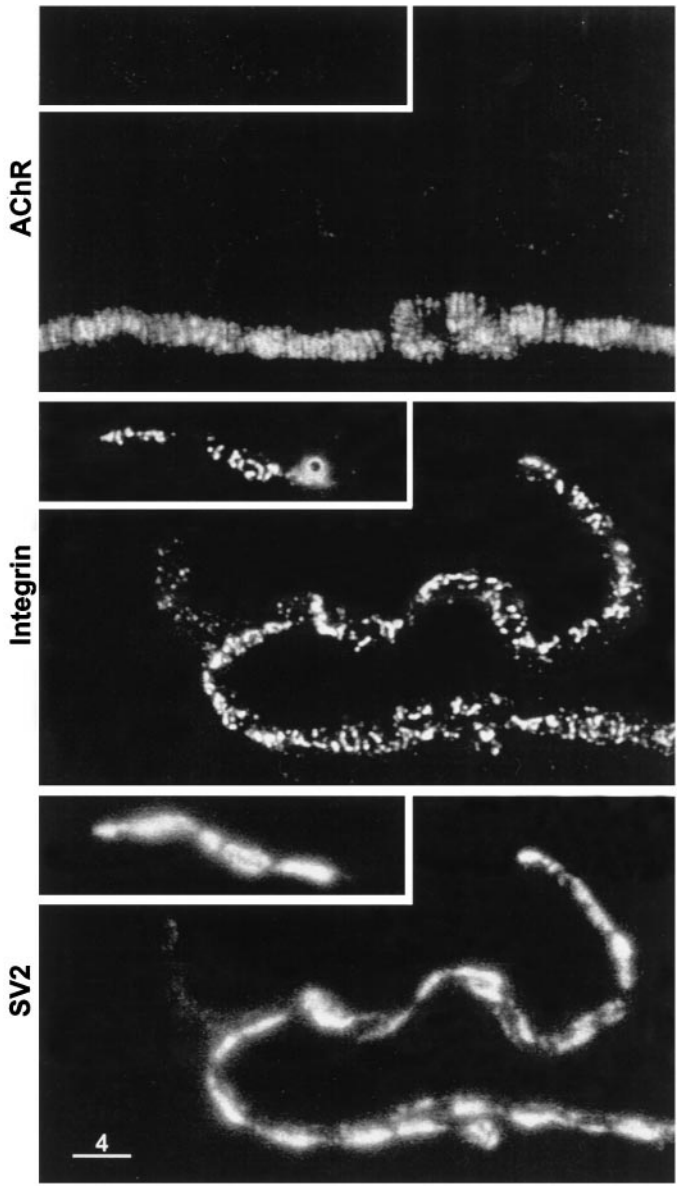


*Figure 6.* Higher magnification view of framed portions of Figure 5. *Top panels,* AChR stain; *middle panels,* $\alpha 3\beta 1$ integrin stain; *bottom panels,* SV2 stain. Note that in the region where the nerve terminal was still present at the postsynaptic membrane, the collagenase treatment partially disrupted the integrin bands and altered their orientation such that many of them were no longer aligned with the AChR bands. A similar disorganization of the integrin bands is apparent along the displaced portions of the nerve terminal. Scale bar, 4 $\mu$m.

of enzyme-treated neuromuscular junctions. Similar results were obtained when mAb P7A12 was used instead of mAb P2A5. Taken together, these observations indicate that the $\alpha 3\beta 1$ integrin bands are associated with the active zones of motor nerve terminals.

Further confirmation of this conclusion was obtained by comparing the distribution of presynaptic N-type calcium channels, known to be located at the active zones of frog motor nerve terminals (Robitaille et al., 1990; Cohen et al., 1991), with the disorganized integrin bands after enzymatic treatment. As seen in Figure 8, there was extensive colocalization of the red fluorescence associated with the calcium channels and the green immunofluorescence of the integrin bands. In fact, integrin immunofluorescence was present at all sites of the calcium channel fluorescence (active zones), including those active zones whose shape and orientation were markedly altered by the enzyme treatment. Conversely, calcium channel fluorescence was not detected at other sites of bright integrin immunofluorescence such as the outer surface of terminal Schwann cells (Fig. 8*A, arrow*) or satellite cells. At individual enzyme-altered active zones the integrin immunofluorescence sometimes extended beyond the calcium channel fluorescence (Fig. 8*A*), but this may attributable to the fact that the calcium channel fluorescence was considerably fainter than the integrin immunofluorescence. Alternatively, it may be that there is a more rapid loss of calcium channels than of integrin during the course of active zone disruption. In either case these experiments indicate that $\alpha 3\beta 1$ integrin is present at all active zones where N-type calcium channels are clustered on *Xenopus* motor nerve terminals.

## DISCUSSION

This study has indicated that $\alpha 3\beta 1$ integrin is present on *Xenopus* motor nerve terminals and concentrated at their active zones, the sites of calcium-dependent exocytosis. The evidence that the anti-$\alpha 3\beta 1$ integrin immunofluorescence was associated with active zones can be summarized as follows. Active zones are known to be in spatial register with the postsynaptic junctional folds (Couteaux and Pécot-Dechavassine, 1970; Dreyer et al., 1973) and so too were the synaptic bands of anti-integrin immunofluorescence. After denervation, active zones disappear as the motor nerve terminals degenerate (Ko, 1981), and so too did the synaptic bands of anti-integrin immunofluorescence. When muscles are treated enzymatically to digest the synaptic basal lamina and permit displacement of the motor nerve terminals, the active zones undergo variable degrees of disorganization and disruption (Nystrom and Ko, 1988). Treatment with collagenase led to similar changes in the synaptic integrin bands and, in cases where the motor nerve terminals were displaced from their site of innervation on the muscle cell, the bands were associated with the displaced nerve terminals rather than with the postsynaptic membrane. In addition, combined staining for integrin and for the N-type calcium channel, which is known to be concentrated at active zones on frog motor nerve terminals (Robitaille et al., 1990; Cohen et al., 1991), revealed integrin immunofluorescence at all sites of calcium channel fluorescence even when the orientation and shape of the active zones was altered by collagenase treatment.

That $\alpha 3\beta 1$ integrin is present at active zones on motor nerve terminals is consistent with other findings. Motor neurons express both subunits (Pinkstaff et al., 1998, 1999), and both are detected at the neuromuscular junction (Bozyczko et al., 1989; Belkin et al., 1996; Martin et al., 1996). Moreover, recent evidence indicates that the $\alpha 3$ subunit is associated with the nerve terminals that innervate the electric organ of the marine ray (Sunderland et al., 2000). There is also evidence that the $\alpha 1$ subunit, which is concentrated at the neuromuscular junction, may be associated with the motor nerve terminals (Martin et al., 1996). Active zones may therefore contain more than one type of integrin. The detection of integrins at some nerve terminals in the hippocampus (Nishimura et al., 1998) raises the possibility that active zones elsewhere in the nervous system may also contain integrins.

That $\alpha 3\beta 1$ integrin, and perhaps others, is present on motor nerve terminals and concentrated at active zones suggests a number of functional consequences. One possibility is that pre-

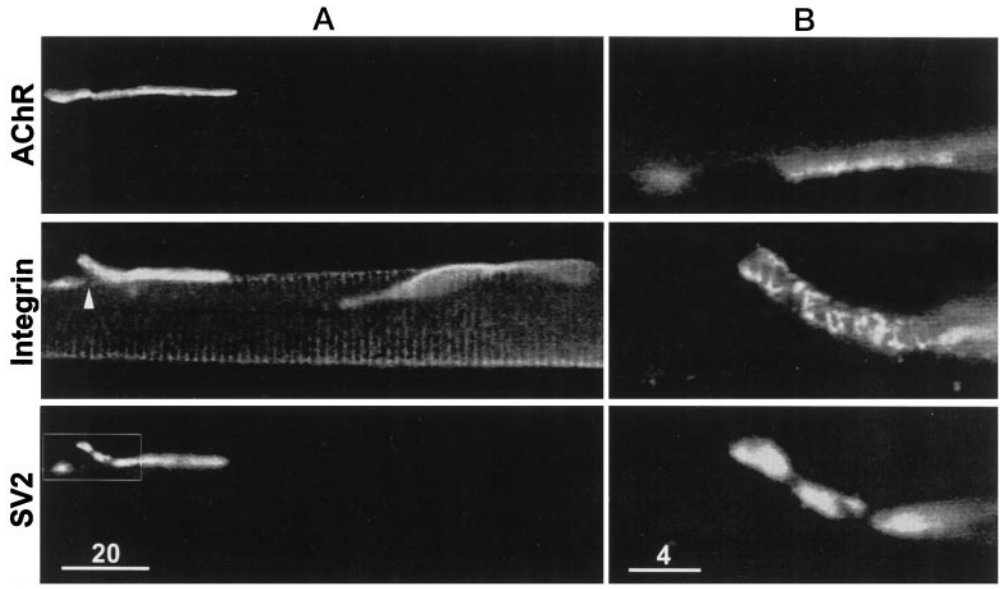


*Figure 7.* Synaptic and nonsynaptic staining patterns after treatment with collagenase. *A,* Low magnification view of AChR stain (*top panel*), $\alpha 3\beta 1$ integrin stain (*middle panel*), and SV2 stain (*bottom panel*). The framed portion of the field (*bottom panel*) contains a neuromuscular junction and a displaced nerve terminal. Note that integrin stain was associated with the displaced nerve terminal and not with the terminal-free portion of postsynaptic membrane (*middle panel, arrowhead*). The integrin stain also reveals costameres and a satellite cell. *B,* Higher magnification of framed area. Bands of integrin stain are apparent on the displaced nerve terminal. The absence of integrin stain on the terminal-free portion of postsynaptic membrane is also apparent. Scale bars: *A*, 20 $\mu$m; *B*, 4 $\mu$m.

synaptic integrin participates in the adhesion of the motor nerve terminals to the synaptic basal lamina. It is known that $\alpha 3\beta 1$ integrin can interact with laminins and collagens (Hynes, 1992; Clarke and Brugge, 1995; Aplin et al., 1998), and synapse-specific forms of these are present in the basal lamina at the neuromuscular junction (Sanes, 1995; Patton et al., 1997). Moreover, integrins can interact directly with specific cytoskeletal proteins and thereby provide a transmembrane linkage between the basal lamina and cytoskeleton (Hynes, 1992; Clarke and Brugge, 1995; Aplin et al., 1998). The nerve terminals that innervate the electric organ contain the cytoskeletal protein spectrin which, based on immunoprecipitation, is part of a complex that includes presynaptic calcium channels as well as one of the synaptic laminins but not the $\alpha 3$ integrin subunit (Sunderland et al., 2000). Therefore it remains to be determined whether other cytoskeletal molecules in motor nerve terminals interact with the cytoplasmic domains of $\alpha 3\beta 1$ integrin and how this (and any other presynaptic) integrin is linked to other molecular components of the active zone. Nevertheless, it seems likely that presynaptic integrin contributes to the adhesion of the terminals to the synaptic basal lamina and that the adhesion may be greatest at the active zones.

Specific $\beta 1$ integrins on muscle cells have been implicated in the formation and/or maintenance of AChR clusters (Martin and Sanes, 1997; Burkin et al., 1998). By analogy, presynaptic integrin on motor nerve terminals may play a role in the formation and/or maintenance of active zones. Experiments on the regeneration of motor nerve terminals indicate that molecules associated with the synaptic basal lamina have an inductive role in the formation of active zones (Sanes et al., 1978). Perhaps such molecules interact directly with integrins on the nerve terminals to trigger a signaling cascade that initiates the clustering of active zone proteins. Presynaptic integrin might also play a structural role by contributing to the molecular scaffold to which active zone proteins are recruited. Such roles in the formation and maintenance of active zones would likewise be relevant to the growth and plasticity of synapses in the adult nervous system. Some of the differences in the congruity between the integrin and AChR bands in Figure 2 may reflect some ongoing growth and/or plasticity of the active zones.

Another potential role for the integrin at active zones is participation in one or more of the steps involved in calcium-dependent exocytosis of neurotransmitter. Current models suggest that nerve terminal membrane proteins such as syntaxin, SNAP-25, and RIM interact with proteins on the surface of the synaptic vesicles, directly or indirectly, to permit targeting of synaptic vesicles to the active zone, docking of the synaptic vesicle at that site, and the subsequent fusion of the synaptic vesicle membrane with that of the nerve terminal (Calakos and Scheller, 1996; Geppert and Südhof, 1998; Sunderland et al., 2000). It may be that the integrins at active zones participate in some of these steps. Such interactions would most probably involve the cytoplasmic domains of the integrins. It will therefore be of interest to determine if integrins do in fact interact with synaptic vesicle proteins or modulate their interaction with other nerve terminal proteins at the active zone.

The presence of integrins on terminal Schwann cells may also be consequential for synaptic structure and function. Schwann cells respond to nerve and muscle damage, act as a guide for nerve sprouts and regenerating nerve terminals, and can influence the stability of the developing neuromuscular junction (Birks et al., 1960b; Son et al., 1996; Trachtenberg and Thompson, 1997; Sanes and Lichtman, 1999). They also respond to synaptic activity and in turn can modulate neurotransmitter release from the terminals (Robitaille, 1998). The magnitudes of such interactions likely depend on how close the terminal Schwann cell is positioned to the source of the nerve-derived (and muscle-derived) activating factors. In terms of this spatial relationship, it is interesting to note that the entry of terminal Schwann cells into the synaptic cleft is inhibited by laminin 11 and perhaps other components of the synaptic basal lamina, thereby

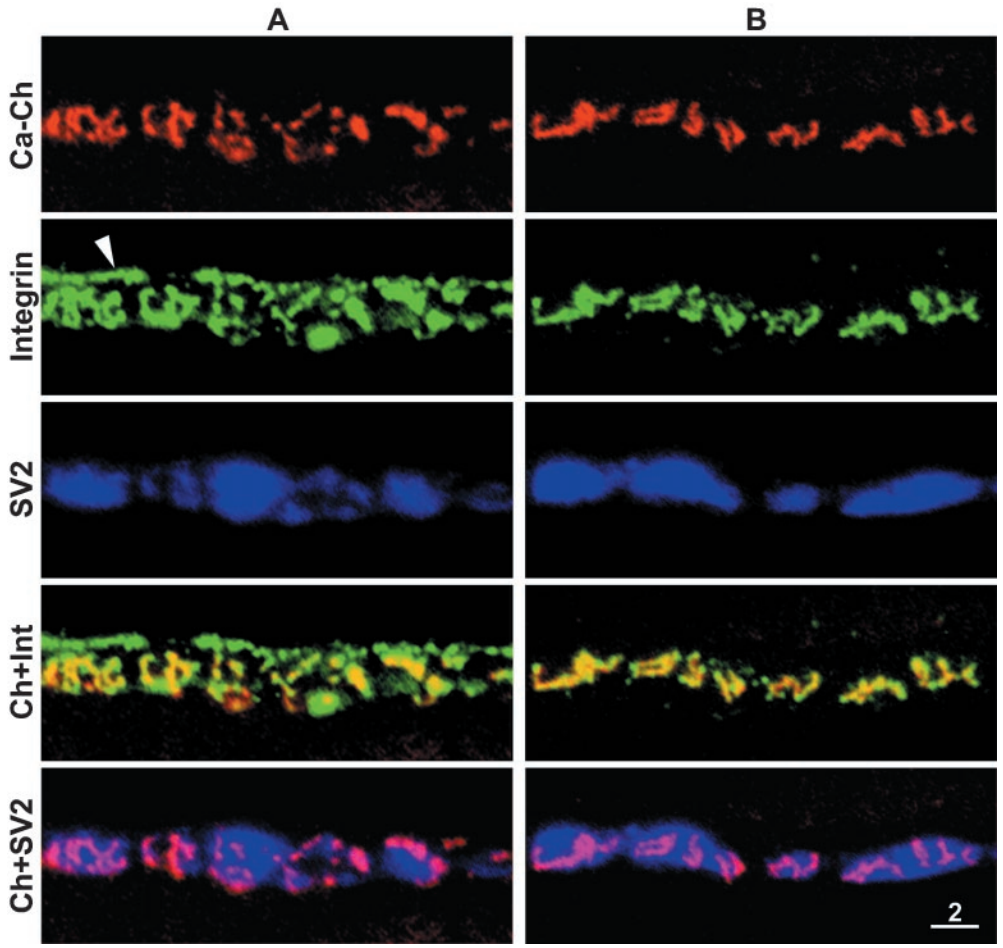


*Figure 8.* Active zones altered by collagenase treatment contain $\alpha 3\beta 1$ integrin. *A, B,* Two different examples. Panels from *top* to *bottom,* Calcium channels at active zones stained with RωCT; $\alpha 3\beta 1$ integrin stain; SV2 stain; merge of calcium channel and $\alpha 3\beta 1$ integrin images; and merge of calcium channel and SV2 images. Integrin stain is present at all active zones revealed by the calcium channel stain, including those whose orientation and shape was altered by the collagenase treatment. Conversely, calcium channel stain was not detected at sites of integrin immunofluorescence that were associated with the terminal Schwann cell (*A, arrowhead*). Scale bar, 2 μm.

defining the limits of intimate apposition between the nerve terminal and Schwann cell (Patton et al., 1998). Schwann cell integrins may be the receptors for this inhibitory interaction. Our findings indicate that terminal Schwann cells express more $\alpha 5\beta 1$ integrin on their surface than the nerve terminals (Table 1). This and/or other differences in their integrin composition may be at least part of the reason why Schwann cells are less adherent to the synaptic basal lamina and do not fully enwrap the nerve terminals. Thus, the integrin composition of the terminal Schwann cells may be important in determining the boundaries of their intimate apposition with the nerve terminals and hence the magnitude of their interactions with the nerve terminals and muscle cells. Additionally, if integrin expression in terminal Schwann cells is affected by the state of the nerve terminals and muscle cells, this would contribute further to their modulation of synaptic structure and function.

## REFERENCES

Anderson MJ, Cohen MW (1974) Fluorescent staining of acetylcholine receptors in vertebrate skeletal muscle. J Physiol (Lond) 237:385–400.

Anderson MJ, Shi ZQ, Zackson SL (1996) Proteolytic disruption of laminin-integrin complexes on muscle cells during synapse formation. Mol Cell Biol 16:4972–4984.

Aplin AE, Howe A, Alahari SK, Juliano RL (1998) Signal transduction and signal modulation by cell adhesion receptors: the role of integrins, cadherins, immunoglobulin-cell adhesion molecules, and selectins [Review]. Pharmacol Rev 50:197–263.

Astrow SH, Qiang H, Ko CP (1998) Perisynaptic Schwann cells at neuromuscular junctions revealed by a novel monoclonal antibody. J Neurocytol 27:667–681.

Bahr B, Staubli U, Xiao P, Chun D, Ji Z, Esteban E, Lynch G (1997) Arg-Gly-Asp-Ser-selective adhesion and the stabilization of long-term potentiation: pharmacological studies and the characterization of a candidate matrix receptor. J Neurosci 17:1320–1329.

Belkin AM, Zhidkova NI, Balzac F, Altruda F, Tomatis D, Maier A, Tarone G, Koteliansky VE, Burridge K (1996) Beta 1D integrin displaces the beta 1A isoform in striated muscles: localization at junctional structures and signaling potential in nonmuscle cells. J Cell Biol 132:211–226.

Betz W, Sakmann B (1973) Effects of proteolytic enzymes on function and structure of frog neuromuscular junctions. J Physiol (Lond) 230:673–688.

Birks R, Huxley HE, Katz B (1960a) The fine structure of the neuromuscular junction of the frog. J Physiol (Lond) 150:134–144.

Birks R, Katz B, Miledi R (1960b) Physiological and structural changes at the amphibian neuromuscular junction, in the course of nerve degeneration. J Physiol (Lond) 150:145–168:145–168.

Blaschuk KL, Guerin C, Holland PC (1997) Myoblast alpha v beta3 integrin levels are controlled by transcriptional regulation of expression of the beta3 subunit and down-regulation of beta3 subunit expression is required for skeletal muscle cell differentiation. Dev Biol (Orlando) 184:266–277.

Bozyczko D, Decker C, Muschler J, Horwitz AF (1989) Integrin on developing and adult skeletal muscle. Exp Cell Res 183:72–91.
Burkin DJ, Gu M, Hodges BL, Campanelli JT, Kaufman SJ (1998) A functional role for specific spliced variants of the alpha7beta1 integrin in acetylcholine receptor clustering. J Cell Biol 143:1067–1075.
Calakos N, Scheller RH (1996) Synaptic vesicle biogenesis, docking, and fusion: a molecular description [Review]. Physiol Rev 76:1–29.
Chen BM, Grinnell AD (1995) Integrins and modulation of transmitter release from motor nerve terminals by stretch. Science 269:1578–1580.
Clark EA, Brugge JS (1995) Integrins and signal transduction pathways: the road taken [Review]. Science 268:233–239.
Cohen MW, Jones OT, Angelides KJ (1991) Distribution of $Ca^{2+}$ channels on frog motor nerve terminals revealed by fluorescent omega-conotoxin. J Neurosci 11:1032–1039.
Couteaux R, Pécot-Dechavassine M (1970) Vesicules synaptiques et poches au niveau des "zones actives" de la jonction neuromusculaire. Comptes Rendus Hebdomadaires des Seances de l' Academie des Sciences - D: Sciences Naturelles 271:2346–2349.
Dodd J, Jessell TM (1988) Axon guidance and the patterning of neuronal projections in vertebrates [Review]. Science 242:692–699.
Dreyer F, Peper K, Akert K, Sandri C, Moor H (1973) Ultrastructure of the "active zone" in the frog neuromuscular junction. Brain Res Dev Brain Res 62:373–380.
Einheber S, Schnapp LM, Salzer JL, Cappiello ZB, Milner TA (1996) Regional and ultrastructural distribution of the alpha 8 integrin subunit in developing and adult rat brain suggests a role in synaptic function. J Comp Neurol 370:105–134.
Gawantka V, Ellinger-Ziegelbauer H, Hausen P (1992) Beta 1-integrin is a maternal protein that is inserted into all newly formed plasma membranes during early *Xenopus* embryogenesis. Development 115:595–605.
Gawantka V, Joos TO, Hausen P (1994) A beta 1-integrin associated alpha-chain is differentially expressed during *Xenopus* embryogenesis. Mech Dev 47:199–211.
Geppert M, Südhof TC (1998) RAB3 and synaptotagmin: the yin and yang of synaptic membrane fusion [Review]. Annu Rev Neurosci 21:75–95.
Hens MD, DeSimone DW (1995) Molecular analysis and developmental expression of the focal adhesion kinase pp125FAK in *Xenopus laevis*. Dev Biol (Orlando) 170:274–288.
Hynes RO (1992) Integrins: versatility, modulation, and signaling in cell adhesion [Review]. Cell 69:11–25.
Joos TO, Whittaker CA, Meng F, DeSimone DW, Gnau V, Hausen P (1995) Integrin alpha 5 during early development of *Xenopus laevis*. Mech Dev 50:187–199.
Kil SH, Lallier T, Bronner-Fraser M (1996) Inhibition of cranial neural crest adhesion in vitro and migration in vivo using integrin antisense oligonucleotides. Dev Biol (Orlando) 179:91–101.
Ko CP (1981) Electrophysiological and freeze-fracture studies of changes following denervation at frog neuromuscular junctions. J Physiol (Lond) 321:627–639.
Martin PT, Sanes JR (1997) Integrins mediate adhesion to agrin and modulate agrin signaling. Development 124:3909–3917.
Martin PT, Kaufman SJ, Kramer RH, Sanes JR (1996) Synaptic integrins in developing, adult, and mutant muscle: selective association of alpha1, alpha7A, and alpha7B integrins with the neuromuscular junction. Dev Biol (Orlando) 174:125–139.
McMahan UJ, Spitzer NC, Peper K (1972) Visual identification of nerve terminals in living isolated skeletal muscle. Proc R Soc London B Biol Sci 181:421–430.
Meng F, Whittaker CA, Ransom DG, DeSimone DW (1997) Cloning and characterization of cDNAs encoding the integrin alpha2 and alpha3 subunits from *Xenopus laevis*. Mech Dev 67:141–155.
Nishimura SL, Boylen KP, Einheber S, Milner TA, Ramos DM, Pytela R (1998) Synaptic and glial localization of the integrin alphavbeta8 in mouse and rat brain. Brain Res Dev Brain Res 791:271–282.
Nystrom RR, Ko CP (1988) Disruption of active zones in frog neuromuscular junctions following treatment with proteolytic enzymes. J Neurocytol 17:63–71.
Patton BL, Miner JH, Chiu AY, Sanes JR (1997) Distribution and function of laminins in the neuromuscular system of developing, adult, and mutant mice. J Cell Biol 139:1507–1521.
Patton BL, Chiu AY, Sanes JR (1998) Synaptic laminin prevents glial entry into the synaptic cleft. Nature 393:698–701.
Pinkstaff JK, Lynch G, Gall CM (1998) Localization and seizure-regulation of integrin beta 1 mRNA in adult rat brain. Brain Res Dev Brain Res Mol Brain Res 55:265–276.
Pinkstaff JK, Detterich J, Lynch G, Gall CM (1999) Integrin subunit gene expression is regionally differentiated in adult brain. J Neurosci 19:1541–1556.
Reichardt LF, Tomaselli KJ (1991) Extracellular matrix molecules and their receptors: functions in neural development [Review]. Annu Rev Neurosci 14:531–570.
Robitaille R (1998) Modulation of synaptic efficacy and synaptic depression by glial cells at the frog neuromuscular junction. Neuron 21:847–855.
Robitaille R, Adler EM, Charlton MP (1990) Strategic location of calcium channels at transmitter release sites of frog neuromuscular synapses. Neuron 5:773–779.
Sanes JR (1995) The synaptic cleft of the neuromuscular junction. Semin Dev Biol 6:163–173.
Sanes JR, Lichtman JW (1999) Development of the vertebrate neuromuscular junction [Review]. Annu Rev Neurosci 22:389–442.
Sanes JR, Marshall LM, McMahan UJ (1978) Reinnervation of muscle fiber basal lamina after removal of myofibers. Differentiation of regenerating axons at original synaptic sites. J Cell Biol 78:176–198.
Son YJ, Trachtenberg JT, Thompson WJ (1996) Schwann cells induce and guide sprouting and reinnervation of neuromuscular junctions [Review]. Trends Neurosci 19:280–285.
Stäubli U, Chun D, Lynch G (1998) Time-dependent reversal of long-term potentiation by an integrin antagonist. J Neurosci 18:3460–3469.
Sunderland WJ, Son Y-J, Miner JH, Sanes JR, Carlson S (2000) The presynaptic calcium channel is part of a transmembrane complex linking a synaptic laminin ($a4\beta2\gamma1$) with non-erythroid spectrin. J Neurosci 20:1009–1019.
Towbin H, Staehelin T, Gordon J (1979) Electrophoretic transfer of proteins from polyacrylamide gels to nitrocellulose sheets: procedure and some applications. Proc Natl Acad Sci USA 76:4350–4354.
Trachtenberg JT, Thompson WJ (1997) Nerve terminal withdrawal from rat neuromuscular junctions induced by neuregulin and Schwann cells. J Neurosci 17:6243–6255.
Wayner EA, Carter WG (1987) Identification of multiple cell adhesion receptors for collagen and fibronectin in human fibrosarcoma cells possessing unique alpha and common beta subunits. J Cell Biol 105: 1873–1884.